Development of a New Isogenic Cell-Xenograft System for Evaluation of NAD(P)H:Quinone Oxidoreductase-Directed Antitumor Quinones: Evaluation of the Activity of RH1

Donna L. Dehn, Shannon L. Winski, and David Ross

Department of Pharmaceutical Sciences, School of Pharmacy and Cancer Center, University of Colorado Health Sciences Center, Denver, Colorado

ABSTRACT

Purpose: The purpose of our study was to develop and validate an isogenic cell line pair that differs only in the expression of NAD(P)H:quinone oxidoreductase (NQO1) that can be used to examine the *in vitro* and *in vivo* role of NQO1 in the bioactivation of the antitumor quinone RH1 (2,5-diaziridinyl-3-(hydroxymethyl)-6-methyl-1,4-benzoquinone), a compound currently in Phase I clinical trials.

Experimental Design: MDA-MB-468 (MDA468) human breast adenocarcinoma cells, homozygous for a polymorphism in NQO1 (*NQO1*2/*2*) and with low levels of NQO1 activity, were stably transfected with human NQO1 to generate a clone (NQ16) expressing very high NQO1 activity. We examined levels of other reductases and looked at biochemical systems that might influence response to antitumor quinones to validate that the isogenic cell line pair differed only in the expression of NQO1. The 3-(4,5-dimethylthiazol-2,5-diphenyl)tetrazolium (MTT) assay was used to determine the differential toxicity of various quinones, including the most recent NQO1-directed antitumor quinone, RH1, between the two cell lines. Human tumor xenografts were established from both MDA468 and NQ16 cells, and the antitumor activity of RH1 was evaluated.

Results: Levels of cytochrome P450 reductase, cytochrome b_5 reductase, soluble thiols, and superoxide dismutase in the NQ16 line were unchanged from the parental line. The functional significance of wild-type NQO1 expression was confirmed by measurement of the differential toxicity of compounds activated or deactivated by NQO1 in the two cell lines. The toxicity of the NQO1-directed antitumor quinones RH1 and streptonigrin were markedly greater and the toxicity of menadione, which is detoxified by NQO1, was ameliorated in the NQ16 line. High levels of NQO1 expression were observed throughout xenograft tumors established from the NQ16 cell line. RH1 treatment was effective at statistically reducing tumor volume in NQ16 xenografts at all of the doses tested [0.1, 0.2, 0.4 mg/kg every day for 5 days), whereas only the highest dose of RH1 resulted in a significant reduction in tumor volume in MDA468 xenografts.

Conclusions: The MDA468/NQ16 isogenic cell line pair is a useful model system for evaluating the role of NQO1 in the bioactivation of antitumor quinones in both cell lines and xenografts. In addition, our data demonstrate that the novel antitumor quinone RH1, is effectively activated by NQO1 both *in vitro* and *in vivo*.

INTRODUCTION

Studies assessing the role of NAD(P)H:quinone oxidoreductase (NQO1) in the bioactivation of antitumor quinones have primarily been carried out in tumor cell lines expressing low and high NQO1 activity (1–4) or in tumor cell line panels in which drug sensitivity was correlated to NQO1 expression retrospectively (5, 6). Results with different cells lines are confounded by genotypic differences such as differential activities of other reductases and different response mechanisms to stress. Bioreductive activation is a complex process and teasing out the contribution of a single reductase requires controlling as many variables as possible. The *NQO1*2/*2* polymorphism (7, 8) is a point mutation (C609T) in the human NQO1 gene that results in a protein reported to have no NQO1 activity because of rapid proteasomal degradation of the NQO1*2 protein (9). Cell lines homozygous for this polymorphism have been used as a molecular tool to develop isogenic cell lines that differ only in their expression of wild-type NQO1. Isogenic cell lines are useful for assessing the role of NQO1 in the bioactivation of antitumor quinones.

We have previously described one isogenic cell line pair, the human BE colon adenocarcinoma cell line (genotyped *NQO1*2/*2*) and its wild-type NQO1 expressing isogenic clone BE NQ-7, with respect to the levels of NQO1 and other reductases and differences in susceptibility to NQO1 substrates (10). The BE/BE NQ7 isogenic pair has only been used for *in vitro* studies and was found to be unsuitable for *in vivo* studies because of an extremely slow growth rate (data not shown). Sharp *et al.* (11) also generated an isogenic pair of cell lines differing only in NQO1 activity using the BE colon cancer cell

line as a parental cell line but using a different expression plasmid. Sharp *et al.* (11) used these lines to generate xenograft tumors but found a substantial decrease in tumor NQO1 activity (from 1400 in cells to 6.2 nmol cytochrome *c* reduced/min/mg protein in tumor homogenates) concomitant with tumor growth. Other investigators have observed the same phenomenon; NQO1 expression decreased in cells when grown as solid tumor xenografts (12).

We developed another isogenic cell line pair using the MDA-MB-468 (MDA468) human ductal breast carcinoma cell line. We report on the characterization of this cell line pair in terms of levels of NQO1 and other reductases, cellular levels of nonprotein thiols and of superoxide dismutase to verify that the isogenic pair of cell lines had similar abilities to respond to alkylating and oxidative stress. The characterization of the cell line pair was completed by assessing the functional significance of wild-type NQO1 expression by comparing the toxicity of compounds that are either activated or deactivated by NQO1 in both cell lines.

We performed initial *in vivo* testing of the MDA468 transfected cell line (NQ16) to evaluate tumorigenicity, wild-type NQO1 protein expression and histological similarities to the human tumor from which the cell line was derived. Xenograft tumors originating from the MDA468 parental line and its isogenic line NQ16, differing only in the expression of NQO1, were used to examine the role of NQO1 in the *in vivo* bioactivation of the antitumor quinone RH1 (2,5-diaziridinyl-3-(hydroxymethyl)-6-methyl-1,4-benzoquinone), a compound currently in Phase I clinical trials.

MATERIALS AND METHODS

Materials. Cytochrome *c*, 2,6-dichlorophenol-indophenol (DCPIP), dicoumarol, 5,5′-dithio-bis(2-nitrobenzoid acid) (Ellman's reagent), glutathione, menadione, 3-(4,5-dimethylthiazol-2,5-diphenyl)tetrazolium (MTT), NADH, streptonigrin (SN), trichloroacetic acid and all other chemicals were purchased from Sigma Chemical Co. (St. Louis, MO). RH1 was synthesized as described previously (10) with stock solutions made up in DMSO. Precast Cambrex PAGEr GOLD 12% Tris glycine minigels and Millipore Immobilon-P PVDF 0.45 μm transfer membranes were purchased from Fisher Scientific (Pittsburgh, PA). Cell culture medium, supplements, and neomycin were obtained from Life Technologies, Inc. (Grand Island, NY) unless otherwise specified. Fetal bovine serum was purchased from Gemini BioProducts, Inc. Mouse antihuman NQO1 primary antibody was derived from hybridoma clones (clones A180 and B771 mixed 1:1) that are maintained by University of Colorado core facilities. All secondary antibodies were from Jackson Immuno Research Laboratories (West Grove, PA). Matrigel was purchased from Collaborative Biomedical Products (Bedford, MA).

Tissue Culture and Transfection. The human breast cancer cell line MDA-MB-468 (MDA468) was obtained from American Tissue Culture Collection (Manassas, VA). Cells were grown as monolayers in RPMI supplemented with 20% fetal bovine serum, 2 mM L-glutamine, 100 units/ml penicillin, and 100 μg/ml streptomycin (complete medium) at 37°C in a humidified atmosphere with 5% CO_2.

MDA468 human breast cancer cells were stably transfected by electroporation with the cytomegalovirus-driven mammalian expression vector pcDNA3.0 containing human wild-type NQO1 cDNA as described previously (10). Selection of transfected cells was achieved with the addition of neomycin to the growth medium. Neomycin-resistant clones were visible after 7–14 days. Colonies were picked and subcultured into 6-well plates that were then expanded and assayed for NQO1 activity (see immediately below). Colonies demonstrating NQO1 activity were taken out of selection and monitored for continued NQO1 expression. Immunoblot analysis as described previously (13) was used to confirm increased NQO1 protein levels. In addition, PCR-RFLP was used to confirm the presence of *NOQ1*2* and wild-type alleles in selected clones as described previously (8).

Enzyme Activity Assays. NQO1 activity was measured as the rate of dicoumarol-inhibitable DCPIP reduction in cell cytosolic samples as described previously (14) with modifications (15) and was normalized to total cytosolic protein (16). Cytochrome P450 reductase was measured in cellular samples as the NAD(P)H-dependent reduction of cytochrome *c* (17). The activity of cytochrome b_5 reductase was measured as the NADH-dependent reduction of cytochrome *c* (18).

Soluble Thiols. Soluble thiols were determined (19) with modifications as described. Briefly, cells were grown to 80% confluence, medium was aspirated, cells were rinsed with PBS, lifted with trypsin/EDTA, and neutralized with complete medium. The cell suspension was vortexed, and 1-ml aliquots were distributed into two tubes on ice. Cells were centrifuged, rinsed in PBS, and recentrifuged. The pellets were either brought up in Buffer A [25 mM Tris-HCl (pH 7.4), 250 mM sucrose containing 5 μM flavin dinucleotide] and sonicated for determination of protein concentration as described previously (16) or were lysed in 5% trichloroacetic acid, vortexed immediately, and centrifuged to pellet cellular protein. The acidified supernatant was mixed with 0.4 M Tris-HCl (pH 8.9), and 5,5′-dithio-bis(2-nitrobenzoid acid) was added to a final concentration of 100 μM. Absorbance at 412 nm was determined, and results were expressed as nanomoles of acid-soluble thiols per mg protein calculated on the basis of a μM glutathione calibration curve.

Growth Inhibition Assays. Toxicity was determined by growth inhibition (MTT) assays as described previously (20).

Alkaline Comet Assay. DNA damage was evaluated by the single-cell gel electrophoresis method, commonly known as the alkaline comet assay, as described previously (20), including modifications by Ward *et al.* (21) to detect DNA cross-linking. A minimum of 200 comets on each slide were visually scored as belonging to one of four classes according to the degree of DNA damage observed, in a similar fashion to the method of other investigators (22–24). Slides were scored blinded. Comet classes are as follows: class 0, intact, well-defined nucleus, no DNA damage; class 1, defined nucleus with light tail formation, <25% DNA in the tail; class 2, defined nucleus but weak fluorescence with 25 and 75% DNA in the tail; class 3, nucleus no longer well defined and tail consists of more than 75% of the DNA.

The visual classification system was verified independently using Euclid Comet Analysis software (St. Louis, MO) from images captured with a Nikon Coolpix 990 digital camera

mounted to the microscope. The total number of comets in classes 0 and 1 (less than 25% DNA in the tail) and in classes 2 and 3 (greater than 25% DNA in the tail) were summed and expressed as a percentage of the total comets counted for each slide.

Establishment of Xenograft Tumors. All of the experiments involving animals were approved by the University of Colorado Health Sciences Center Animal Care and Use Committee and were carried out according to approved protocols. Female athymic nude mice (NCr nu/nu; National Cancer Institute, Fredrick, MD) were received at 5–6 weeks of age and were allowed to acclimate for 2 weeks in sterile microisolator cages with constant temperature and humidity. Mice had free access to food and water. After inoculation with tumor cells, mice were monitored daily and were weighed twice weekly; digital caliper (Mitutoyo, Japan) measurements began when tumors were visible.

***In Vivo* Model Development.** Cells in log phase growth were harvested on the day of use and were injected s.c. at a concentration of 1×10^6 (left shoulder), 2×10^6 (right shoulder and left flank), and 4×10^6 cells (right flank) with 0.1 ml of a 75:25 unsupplemented medium/Matrigel suspension to define the concentration of cells necessary to initiate tumor growth. NQO1 activity in tumor homogenates was measured as described above. Tissue sections (4 μm) were cut from formalin-fixed, paraffin-embedded blocks and were stained as described below (see "Immunohistochemistry").

RH1 Antitumor Activity. Cells in log phase growth were harvested on the day of injection and an equal number of animals were inoculated s.c. bilaterally in the flanks with 0.1 ml of a 75:25 unsupplemented media/Matrigel suspension containing 4×10^7 cells/ml MDA468 or NQ16 cells. When tumors had grown to ~200 mm³ (4 weeks after cell implantation), animals bearing bilateral tumors were randomized into a control and three drug-treatment groups of seven to eight animals per cell line. RH1 (stock solution in DMSO) was diluted into sterile saline just before i.p. injection (0.1 mg/kg, 0.2 mg/kg, or 0.4 mg/kg) daily for five consecutive days (every day for 5 days) The doses of RH1 and schedule of treatment used in this study were based on the maximum tolerated dose (0.45 mg/kg/day i.p., every day for 5 days) as determined by the National Cancer Institute in their xenograft studies.[1] Control animals received an equal volume of DMSO in sterile saline.

Tumor volume was calculated by the formula $L \times W^2/2$ (25), where L is the longer measurement of the tumor and W is the smaller tumor measurement. The increase in tumor volume from the start of treatment (V_0) until the value at any give time (V_t) was calculated for each tumor and was expressed as the relative tumor volume (V_t/V_0) on the day of measurement. The mean of these values was used to calculate the ratio between treated (T) and control (C) tumors (T/C × 100%) as an indication of drug efficacy. Growth inhibition is expressed as 100% − (T/C × 100%). Optimal values are the lowest percentage T:C or the highest growth inhibition reached on a specific day after treatment ended (26). Tumor doubling time (t_D) was calculated

---

Table 1 Average reductase activity

Results are means of a minimum of three independent experiments ±SE.

	Cell lines	
Enzyme	MDA468	NQ16
NQO1[a] (nmol DCPIP/min/mg protein)	9.5 ± 2.2	4797.4 ± 137.5
Cytochrome b_5 reductase (nmol cyt.c/min/mg protein, NADH)	20.4 ± 2.2	20.2 ± 1.9
Cytochrome P450 reductase (nmol cyt.c/min/mg protein, NADPH)	7.0 ± 0.8	6.9 ± 0.6

[a] NQO1, NAD(P)H:quinone oxidoreductase; DCPIP, 2,6-dichlorpheol-indophenol.

by the formula $t_D = t \times [(\log 2)/(\log (V_t/V_0))]$, where V_0 is the tumor volume at the start of treatment, V_t is the tumor volume at time t and t is the time (in days) of the second measurement. Negative values indicate tumor regression (27). Mice were euthanized ~3 months after tumor implantation, and tumors were removed for the determination of NQO1 activity and were paraffin-embedded for histological evaluation.

NQO1 activity was determined after excised tumors were weighed, cut in half, diluted 1:5 in Buffer A, and homogenized on ice for 2 min with a Kontes glass-glass homogenizer. The homogenates were probe sonicated on ice for 30 s, then were centrifuged at $13,000 \times g$ for 10 min. at 4°C. The supernatant was removed and stored at −80°C until activity was measured.

Immunohistochemistry. Xenograft tumor tissue sections (4 μm) were cut from formalin-fixed, paraffin-embedded blocks. H&E staining was performed according to standard histological procedure. Immunodetection of NQO1 was performed as described previously (13) except for the addition of the mouse-on-mouse immunodetection kit according to the manufacturers instructions (Vector, Burlingame, CA).

Statistical Analysis. Statistical analysis was performed using NCSS (Kaysville, UT) software. The two-sample t test was used to evaluate differences between treatment and controls, and Ps < 0.05 were considered significant. Data are presented as mean ± SE.

RESULTS

Characterization of the MDA468 Isogenic Cell Line Pair. A wide range of NQO1 activity was detected in the transfected clones. Activity was continuously measured in transfected clones to ensure maintenance of stable NQO1 expression. The NQ16 clone expressed the highest NQO1 activity level measured and has maintained very high NQO1 activity levels in culture. NQO1 activity levels of parental and transfected NQ16 cells are shown in Table 1. Immunoblot analysis with 5 μg of cell cytosol of the MDA468 parent and the transfected NQ16 cell line demonstrated the presence of NQO1 protein in the transfected NQ16 cells (Fig. 1*A*). PCR-RFLP confirmed the presence of the *NQO1*1* genotype as well as the genomic *NQO1*2* allele in the NQ16 cell line (Fig. 1*B*). NQ16 cells demonstrate both of the DNA sequences, whereas the parental MDA468 cell line has only the *NQO1*2/*2* genotype. Fluorescence *in situ* hybridization (FISH) assays indicated the plasmid
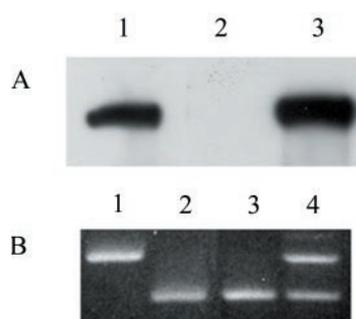
Fig. 1 *A*, the immunoblot for NAD(P)H:quinone oxidoreductase (NQO1) protein. *Lane 1,* 5 ng wild-type recombinant NQO1 protein (standard); *Lane 2,* 5 μg total cytosolic protein from MDA468 cells; *Lane 3,* 5 μg total cytosolic protein from NQ16 cells. *B,* PCR RFLP products. *Lane 1,* wild-type NQO1 standard; *Lane 2, NQO1*2/*2* standard; *Lane 3,* MDA468 cells; *Lane 4,* NQ16 cells. NQ16 cells have both *NQO1*2* and wild-type NQO1 alleles.

containing the wild-type NQO1 cDNA had integrated into chromosome 3 of the NQ16 transfected cells (data not shown). Multiple copies of the gene insert were not detected by fluorescence *in situ* hybridization. To confirm the fluorescence *in situ* hybridization results, real-time PCR (Laragen Inc., Los Angeles, CA) determined that two copies of the wild-type *NQO1* gene were present in the NQ16 cells.

To ensure that transfection of the MDA468 cell line with wild-type NQO1 did not alter biochemical systems that might influence response to antitumor quinones, the enzymatic activity of other reductive enzymes and levels of nonprotein cellular thiols were monitored in the parental MDA468 and transfected NQ16 cells. No statistical difference ($P < 0.05$) was observed in the activities of cytochrome P450 reductase or cytochrome b_5 reductase between the parental MDA468 cells and the NQ16 cells transfected with wild-type NQO1 (Table 1). No significant differences ($P < 0.05$) in total nonprotein cellular thiols, used as an indication of available glutathione, were observed between MDA468 (5.0 ± 0.7 nmol acid-soluble thiols/mg protein) and

NQ16 cells (4.7 ± 0.7 nmol acid-soluble thiols/mg protein). In addition, no apparent differences in levels of cytosolic superoxide dismutase (Cu/Zn superoxide dismutase) protein levels were found by immunoblot using β-actin as a loading control (data not shown).

To ensure that this isogenic cell line pair responded similarly to compounds that were not substrates for NQO1, the toxicity of cisplatin was evaluated in these cell lines. Cisplatin can form inter- and intrastrand cross-links in DNA (28) independent of NQO1 status. No statistical difference was observed in the cytotoxicity of cisplatin to the MDA468 parental cells and the NQ16 NQO1-transfected cells as measured by the MTT assay. The $IC_{50} \pm$ SE for the MDA468 parental line was calculated as 0.57 ± 0.05 μM and 0.54 ± 0.06 μM for the NQ16 cell line. Cisplatin also displayed equivalent DNA cross-linking in both MDA468 and NQ16 cell lines. After treatment with cisplatin (50 μg/ml) and subsequent irradiation, ∼46% of all of the comets counted, in either cell line, retained more than 75% of the DNA in the head of the comet (Fig. 2). This is a 2-to-5-fold increase over the amount of DNA that remained in the head of control cells (after irradiation). Retardation in the amount of DNA migration into the tail of the comet after irradiation is an indication of cross-linked DNA (29).

As a validation of the functional significance of the presence of wild-type NQO1, the toxicity of several compounds known to be substrates of NQO1 were tested in the MDA468/ NQ16 isogenic pair. SN, an aminoquinone antitumor antibiotic, is a highly efficient substrate for NQO1 (30, 31) with cytotoxicity correlated to NQO1 activity (11, 20, 32). SN was significantly ($P < 0.05$) more toxic to NQ16 cells than to the parental MDA468 cells (Table 2). Menadione (2-methyl-1,4-naphthoquinone), a vitamin K3 analog (33) can arylate and undergo one electron reduction resulting in the formation of superoxide anion and hydrogen peroxide as a result of redox cycling. NQO1 plays a protective role in the metabolism of menadione because it prevents the oxidative stress caused by this compound through two-electron reduction to the hydroquinone. Consistent with the role of NQO1 in the detoxification of menadione, it was signif-
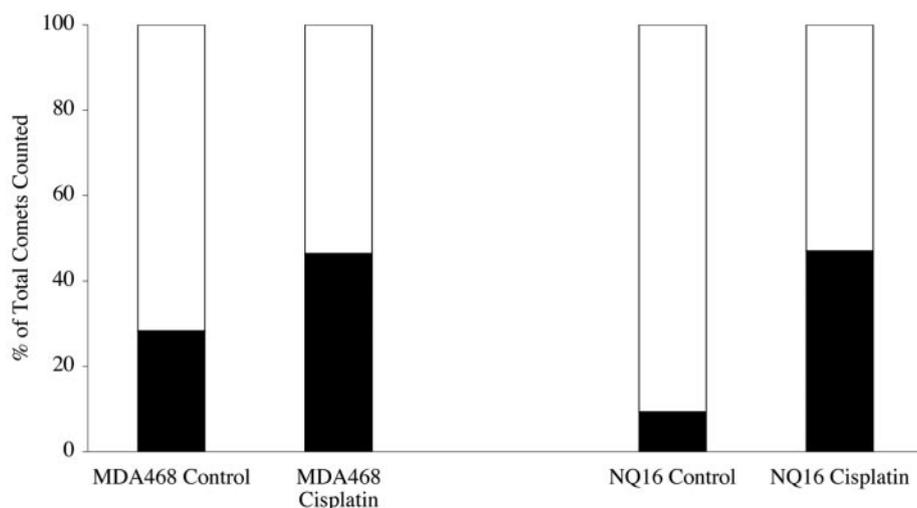

Fig. 2 Percentage of comets formed in each category (*black bars,* <25% DNA in the tail; *white bars,* >25% DNA in the tail) after treatment with cisplatin compared with controls. Both cisplatin-treated and control cells were irradiated with 10 Gy before processing for the comet analysis. Irradiation induces a given amount of strand breaks in both treated and control cells. Broken DNA can migrate into the tail of the comet. Cross-linked DNA will not migrate into the tail and is identified by an increase in the percentage of total comets counted with less than 25% DNA in the tail compared with controls. Two hundred comets were counted per experiment; two separate experiments were conducted.

Table 2 IC$_{50}$s for known NAD(P)H:quinone oxidoreductase (NQO1) substrates

Compound	IC$_{50}$ (nM)	
	MDA468	NQ16
Streptonigrin	212.2 ± 17.4	2.2 ± 1.4[a]
Menadione	5600 ± 1100	9200 ± 1300[a]
RH1	30 ± 2.7	3.2 ± 1.7[a]

[a] A significant difference ($P < 0.05$) between IC$_{50}$s for MDA468 and NQ16 cells.

icantly less toxic ($P < 0.05$; higher IC$_{50}$) to NQ16 cells that express wild-type NQO1 than to MDA468 cells (Table 2). Finally, RH1, the novel antitumor agent developed specifically to be bioactivated by NQO1, was significantly more toxic to NQ16 cells than to the parental MDA468 cells (Table 2). The IC$_{50}$ of RH1 was about 10-fold lower in NQ16 cells that express high levels of wild-type NQO1 protein compared with the IC$_{50}$ for the parental MDA468 cells.

Development of an *in Vivo* Model. The NQ16 stably transfected cell line was found to be tumorigenic in NCr nu/nu mice, exhibiting a doubling time of 7.6 days. NQO1 activity levels *in vivo* (2958.4 ± 92 nmol DCPIP reduced/min/mg protein) were ~77% of those measured in the particular cell culture used for implantation (3856.8 ± 325 nmol DCPIP reduced/min/mg protein). Tumors derived from NQ16 cells (Fig. 3*A*) demonstrated a similar appearance to human breast adenocarcinoma (Fig. 3*B*) with tumor cells disposed in cords embedded in connective tissue and solid tumor cell nests. In addition, immu-

nostaining of tumor tissue for NQO1 protein (Fig. 3*C*) demonstrated relatively even expression of NQO1 in tumor cells.

RH1 Antitumor Activity Studies. Approximately 7 weeks after implantation of MDA468 or NQ16 cells, the majority of tumors of both cell lines had grown to 200 mm^3 and the calculated pretreatment tumor doubling times were similar, 12.9 days for MDA468 tumors and 11.8 days for NQ16 tumors.

RH1 treatment (0.4 mg/kg and 0.2 mg/kg) of mice bearing NQ16 tumors (Fig. 4) resulted in a significant reduction ($P < 0.05$) in tumor volume between treated groups and controls as early as 5 days after the treatment period ended. Low-dose RH1 (0.1 mg/kg) also resulted in a significant reduction in tumor volume between treated mice and controls, although additional time was required (3 days) for the difference to become observable. Complete regression of a single tumor was observed for each of two mice that received high-dose RH1. RH1 exhibited antitumor activity in a dose-dependent manner against NQ16 tumors growing in athymic mice.

High-dose RH1 treatment (0.4 mg/kg) was required to significantly ($P < 0.05$) reduce tumor volume compared with controls in mice bearing MDA468 tumors starting 8 days after the treatment period ended (Fig. 5). RH1 treatment (0.2 mg/kg) produced a significant difference ($P < 0.05$) in tumor volume between treated and control animals at only two individual time points (19 days and 33 days after RH1 treatment was complete), but not at any intervening period. Low-dose RH1 treatment did not significantly reduce the tumor volume in treated mice compared with control mice at any time.

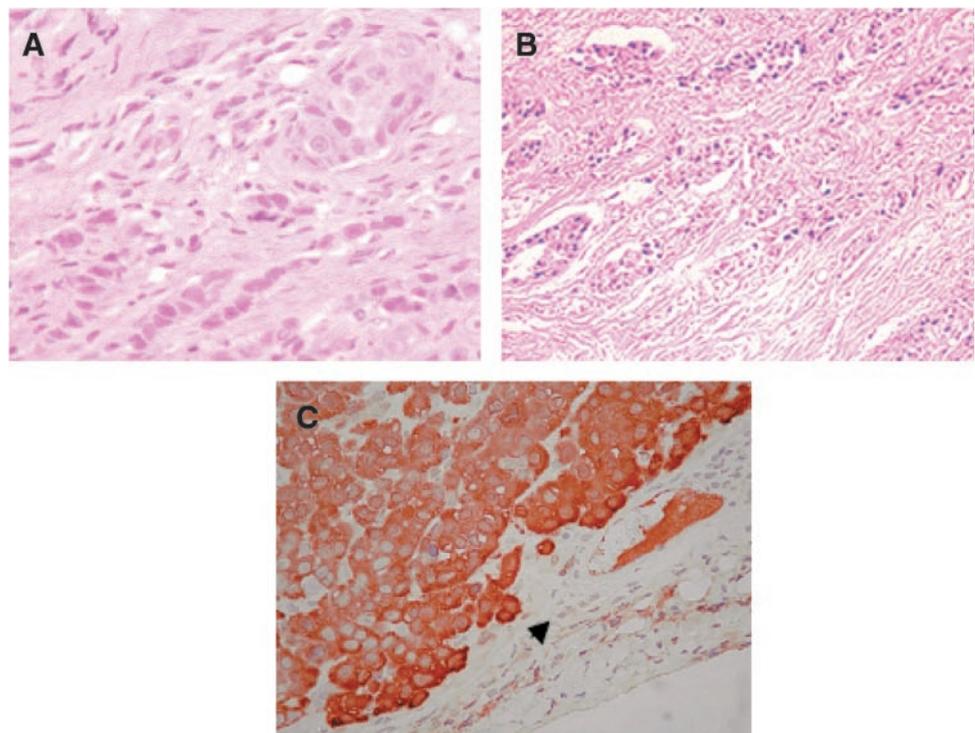The efficacy of RH1 treatment is depicted graphically (Fig.

Fig. 3 Comparison of tumor histology between NQ16 human tumor xenograft section (*A*) and human breast ductal adenocarcinoma (*B*; courtesy of Dr. Kenneth Shroyer, University of Colorado Health Sciences Center, Denver, Colorado), all stained with H&E. There are similarities in cellular architecture with tumor cells dispersed in cords and nests. *C*, NQ16 tumor xenograft section immunostained for NAD(P)H:quinone oxidoreductase (NQO1) protein. *Arrow*, mouse stromal cells that do not stain for NQO1. *A* and *C*, ×200; *B*, ×100.

6, *A–C*) as the percentage treatment:control (T:C) ratio. Fig. 6*A* is a comparison of the efficacy of high-dose RH1 (0.4 mg/kg) in NQ16 tumors and MDA468 tumors. At this dose, the optimal percentage T:C for NQ16 tumors was 10.6% (at day 26 after the end of RH1 treatment) and 24% for MDA468 tumors (day 22). At the medium dose of RH1 (0.2 mg/kg; Fig. 6*B*), an optimal percentage T:C was 41% (day 15) for NQ16 tumors and 52% (day 33) for MDA468 tumors. In NQ16 tumors, the lowest RH1 dose (Fig. 6*C*) resulted in an optimal percentage T:C of 52% (day 26), 20% below the optimal percentage T:C of 74% (at day 26) for MDA468 tumors.

Toxicity Evaluation. Weight loss was used as a surrogate measure for systemic drug toxicity (25, 34). Before initiation of treatment with RH1, weights remained steady in both MDA468 and NQ16 tumor-bearing animals. There were no significant differences in body weight between treated and control MDA468 tumor-bearing animals at any concentration of RH1. A significant decrease in body weight from control animals was observed in all RH1-treated mice bearing NQ16 xenograft tumors 5 weeks after treatment was initiated (1 week before death). Animals lost up to 14% body weight over the period after the initiation of treatment until death, although no toxicity-related deaths occurred (death within 2 weeks of the start of treatment). No signs of overt drug toxicity were seen in any animals.

NQO1 Activity in Tumor Tissue. The activity of NQO1 in tumor homogenates is presented in Table 3. Although the NQO1 activity in NQ16 tumors was less than that measured in NQ16 cells *in vitro*, this cell line displays such high activities that a decrease should have little effect on the levels of enzyme available to activate RH1. No significant differences in NQO1 activity of tumor homogenates between treatments within each cell line was seen.

DISCUSSION

NQO1 has been used as a target for the enzyme-directed approach to the design of antitumor agents because NQO1 is
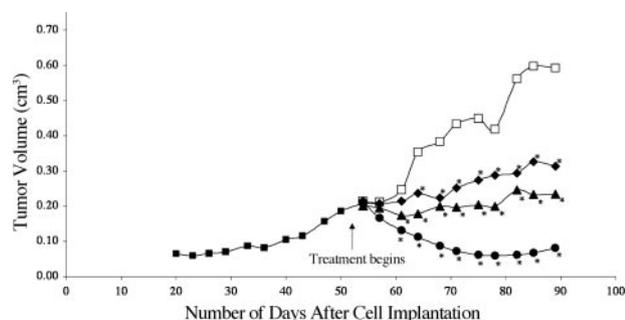

Fig. 5 MDA468 tumor growth depicting measured tumor volume (cm^3) over time. *Each plot point,* represents the mean of all animals in the treatment group (seven to eight). Error bars were omitted for better visual clarity. *Circles,* high-dose RH1 (0.4 mg/kg) treatment group; *triangles,* medium-dose RH1 (0.2 mg/kg) treatment group; *diamonds* low-dose RH1 (0.1 mg/kg) treatment group. □, control animals that received an equivalent volume of DMSO in saline. ∗, the time point when tumor volume in treatment groups was statistically different from controls as determined by the Student's *t* test with equal variance.
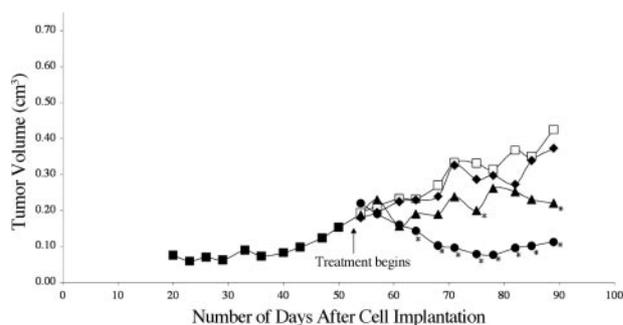
expressed at high levels throughout many human solid tumors (35–38). Various models have been used to study the role of NQO1 in the cytotoxicity of NQO1-directed antitumor agents. Because of the complex nature of quinone bioactivation, an excellent model for *in vitro* and *in vivo* studies is one of an isogenic pair of human cell lines differing only in the expression of wild-type human NQO1. Several such lines have been generated in our laboratory, and the MDA468 human breast adenocarcinoma and its isogenic line, NQ16, were characterized for this study to ensure conformity between them aside from expression of NQO1. The parental cell line is homozygous for the *NQO1*2* polymorphism that results in the production of a mutated form of the NQO1 protein (NQO1*2 protein) which undergoes rapid proteasomal degradation (9). The activity of cytochrome P450 reductase and cytochrome b_5 reductase were similar between the MDA468/NQ16 isogenic pair as were levels of superoxide dismutase and glutathione. These results indicate that the isogenic pair should metabolize quinones and antitumor agents similarly via one electron reductases. Detoxification of reactive electrophiles and superoxide mediated via soluble thiols and superoxide dismutase, respectively, would also be expected to be similar.

Cisplatin was used as part of the validation of the MDA468 isogenic pair of cell lines because its activation and toxicity are independent of NQO1. MDA468 cells and NQ16 cells exhibited similar cytotoxicity and degree of cross-linking of DNA after exposure to cisplatin. In contrast, the isogenic cell line pair exhibited marked differences in toxicity when exposed to NQO1 substrates. Reduction of SN by NQO1 results in an unstable hydroquinone that can react with molecular oxygen to produce reactive oxygen species and regenerate the parent quinone. Hydroxyl radicals are produced in the presence of Cu^{2+} and Fe^{2+} in a Fenton-type reaction that results in single-and double-strand DNA breaks, the ultimate source of cellular damage (39). SN was found to be substantially more toxic to NQ16 cells expressing NQO1 than to MDA468 cells. These results correspond to data obtained by others in which SN was shown to

Fig. 4 NQ16 tumor growth depicting measured tumor volume (cm^3) over time. *Each plot point* represents the mean of all animals in the treatment group (seven to eight). Error bars were omitted for better visual clarity. *Circles,* high-dose RH1 (0.4 mg/kg) treatment group; *triangles,* medium-dose RH1 (0.2 mg/kg) treatment group; *diamonds,* low-dose RH1 (0.1 mg/kg) treatment group. □, control animals that received an equivalent volume of DMSO in saline. ∗, the time point when tumor volume in treatment groups was statistically different from controls as determined by the Student's *t* test with equal variance.
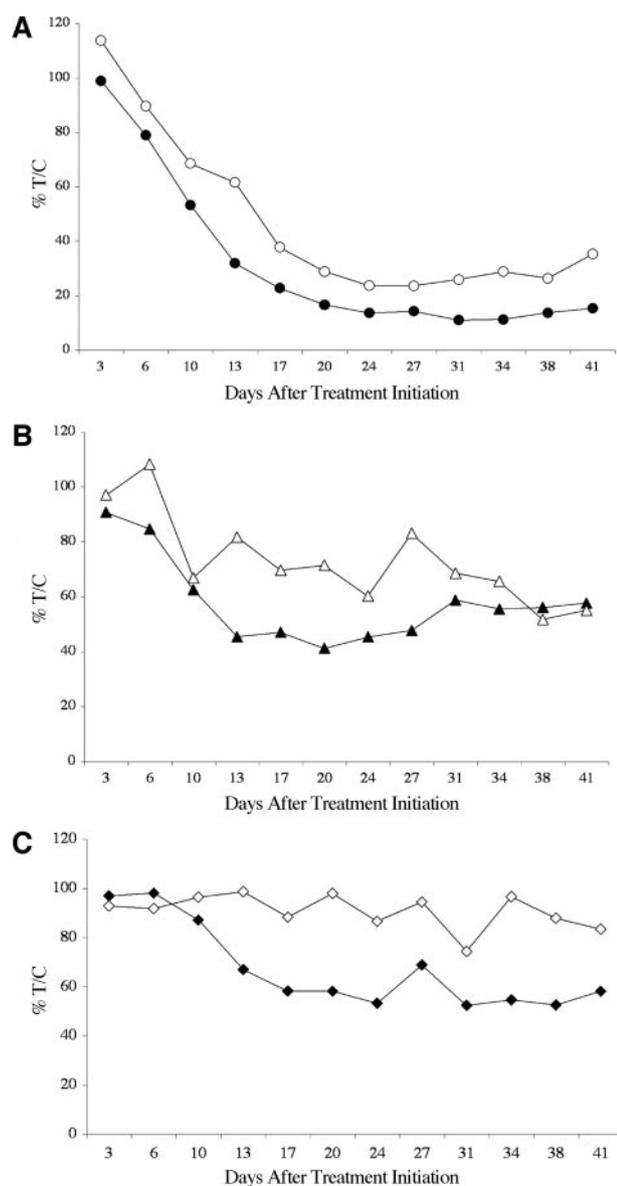
Fig. 6 Efficacy of RH1 treatment in MDA468 tumor xenografts (*open symbols*) and NQ16 tumor xenografts (*filled symbols*). *A*, percentage T:C (% T/C) for high-dose RH1 treatment (0.4 mg/kg, *circles*). Both cell lines show a similar pattern although NQ16 tumors display a ≥10% lower T:C than MDA468 tumors. *B*, percentage T:C (% T/C) for medium-dose RH1 (0.2 mg/kg, *triangles*). *C*, percentage T:C (% T/C) for low-dose RH1 (0.1 mg/kg, *diamonds*) which highlights the difference in RH1 effectiveness between NQ16 tumors and MDA468 tumors.

have the strongest correlation between NQO1 activity levels and toxicity in 31,000 compounds tested (40). Furthermore, SN induced more DNA damage in NQ16 cells than in MDA468 cells as determined by the comet assay (data not shown). Over 99% of the comets formed after SN treatment of NQ16 cells had more than 75% of the DNA in the tail, whereas only about 40% of the comets formed after MDA468 cells were treated with SN had more than 75% of the DNA in the tail. Two-electron reduction of menadione by NQO1 prevents redox cycling that

occurs when menadione undergoes one-electron reduction. In keeping with the protective role of NQO1 in the detoxification of menadione, the transfected NQ16 cells were less sensitive to menadione than were the parental MDA468 cells. Menadione may be a better substrate for one-electron reductases than for NQO1 because the presence of NQO1 in NQ16 cells did not provide a substantial decrease in toxicity compared with the MDA468 cells (1.6-fold). This small difference in toxicity to menadione was also seen by Gustafson *et al.* (41) using Chinese hamster ovary cells transfected with human wild-type NQO1 (1.4-fold difference between isogenic lines). The final compound used to validate the MDA468/NQ16 isogenic cell line model was RH1. RH1 is "activated" upon two-electron reduction of the quinone, and the two aziridinyl functional groups undergo protonation that results in aziridine ring opening. The resulting bifunctional alkylating species can covalently bind to DNA and form inter- and intrastrand cross-links (42). RH1 was more toxic to the NQ16 cell line than to the parental MDA468 cell line, consistent with what was observed in the BE colon carcinoma cells transfected with wild-type NQO1 (10).

We then evaluated the ability of the NQ16 stably transfected cell line to create a competent xenograft model (acceptable growth rate, NQO1 activity, uniform NQO1 expression, and histological characteristics of the xenograft tumor). Tumors that were initiated from NQ16 cells grew slowly but formed well-differentiated tumor architecture that mimicked human breast adenocarcinoma, a characteristic that is desirable for predictive screening of potential anticancer drugs (43). Although the NQ16 tumors had lower NQO1 activity levels than the cell line used to establish them the large differential in NQO1 activity between isogenic lines was retained. The reason for the down-regulation of NQO1 activity in cells grown as solid tumor xenografts is unclear. Tumors with central areas of necrotic cells could have contributed to the dilution of activity levels because of nonexpressing cells.

The *in vivo* evaluation of RH1 validated the *in vitro* studies that showed a difference in sensitivity to RH1 between NQ16 cells and the parental MDA468 cells. A statistically significant and dose-dependent inhibition of tumor growth, as assessed by tumor volume, was demonstrated in NQ16 human tumor xenografts treated with all doses of RH1, and a complete regression of two tumors was observed after treatment at high-dose RH1. In contrast, only at high doses was RH1 effective in arresting tumor growth and reducing tumor volume in MDA468

Table 3 NAD(P)H:quinone oxidoreductase (NQO1) activity in MDA468/NQ16 tumor homogenates

Values are for a minimum of seven to eight animals in each treatment group with activities done in duplicate.

| Treatment | NQO1 activity (nmol DCPIP[a] reduced/min/mg of protein) | |
	MDA468	NQ16
Control	5.7 ± 1.2	2306.0 ± 414.2
Low-dose RH1	5.1 ± 1.2	1843.1 ± 66.4
Medium-dose RH1	11.6 ± 3.0	3048.6 ± 299.3
High-dose RH1	21.3 ± 11.4	2092.3 ± 59.4

[a] DCPIP, 2,6-dichlorophenol-indophenol.

tumor xenografts. One possible explanation for the response of MDA468 tumor xenografts to high-dose RH1 may be the high levels of NQO1*2 protein in MDA468 cells. The MDA468 cells carry four copies of chromosome 16 or its derivates (data not shown) and have the highest amount of NQO1*2 protein of any of the *NQO1*2/*2* cell lines that we have tested. As a result, we were able to detect low levels of NQO1 catalytic activity in parental MDA468 cells (Table 1) and in MDA468 xenograft tumor homogenates (Table 3). These very low activity levels, presumably resulting from high protein levels, may be sufficient to bioactivate extremely efficient substrates such as RH1. Alternately, RH1 may be activated by other one- and two-electron reductases in tumor cells or by mouse NQO1. Phillips *et al.* (44) speculated NQO1 activity measurements in tumor xenograft tissue may not accurately reflect NQO1 activity of the tumor cell due to the contribution of mouse stromal tissue that express NQO1 protein. Mouse NQO1 is very similar to human NQO1 in terms of substrate specificity (45) and could readily bioactivate RH1.

It is also important to note that RH1 was not overtly toxic to mice, using body weight as an indicator of toxicity. Although NQ16 tumor-bearing mice lost body weight, this occurred in the last week of the study. We speculate that weight loss could have resulted from a buildup of unmetabolized or toxic proteins released from tumor cells undergoing apoptosis or necrosis.

In summary, we have demonstrated that the MDA468/NQ16 pair of cell lines represents a useful model system for evaluating the ability of NQO1-directed antitumor quinones in both cell lines and xenografts. Our data also demonstrate increased activity of the antitumor quinone RH1 in both NQ16 cell lines and xenografts, validating the role of NQO1 in the bioactivation of RH1 *in vivo*. These data add to the evidence that NQO1 can be exploited as an activating enzyme for chemotherapeutic quinones.

ACKNOWLEDGMENTS

REFERENCES

1. Siegel D, Gibson NW, Preusch PC, Ross D. Metabolism of mitomycin C by DT-diaphorase: role in mitomycin C-induced DNA damage and cytotoxicity in human colon carcinoma cells. Cancer Res 1990;50: 7483–9.

2. Siegel D, Gibson NW, Preusch PC, Ross D. Metabolism of diaziquone by NAD(P)H:(quinone acceptor) oxidoreductase (DT-diaphorase): role in diaziquone-induce DNA damage and cytotoxicity in human colon carcinoma cells. Cancer Res 1990;50:7293–300.

3. Beall H, Murphy A, Siegel D, Hargreaves R, Butler J, Ross D. Nicotinamide adenine dinucleotide (phosphate): quinone oxidoreductase (DT-diaphorase) as a target for bioreductive antitumor quinones: quinone cytotoxicity and selectivity in human lung and breast cancer cell lines. Mol Pharmacol 1995;48:499–504.

4. Beall HD, Winski S, Swann E, et al. Indolequinone antitumor agents: correlation between quinone structure, rate of metabolism by recombinant human NAD(P)H:quinone oxidoreductase, and in vitro cytotoxicity. J Med Chem 1998;41:4755–66.

5. Fitzsimmons SA, Workman P, Grever M, Paull K, Camalier R, Lewis AD. Reductase enzyme expression across the National Cancer Institute tumor cell line panel: correlation with sensitivity to mitomycin C and EO9. J Natl Cancer Inst (Bethesda) 1996;88:259–69.

6. Mikami K, Naito M, Tomida A, Yamada M, Sirakusa T, Tsuruo T. DT-diaphorase as a critical determinant of sensitivity to mitomycin C in human colon and gastric carcinoma cell lines. Cancer Res 1996;56: 2823–6.

7. Traver RD, Horikoshi T, Danenberg KD, et al. NAD(P)H:quinone oxidoreductase gene expression in human colon carcinoma cells: characterization of a mutation which modulates DT-diaphorase activity and mitomycin sensitivity. Cancer Res 1992;52:797–802.

8. Traver RD, Siegel D, Beall HD, et al. Characterization of a polymorphism in NAD(P)H:quinone oxidoreductase (DT-diaphorase). Br J Cancer 1997;75:69–75.

9. Siegel D, Anwar A, Winski SL, Kepa JK, Zolman KL, Ross D. Rapid polyubiquitination and proteasomal degradation of a mutant form of NAD(P)H:Quinone oxidoreductase 1. Mol Pharmcol 2001;59:263–8.

10. Winski SL, Hargreaves RH, Butler J, Ross D. A new screening system for NAD(P)H:quinone oxidoreductase (NQO1)-directed antitumor quinones: identification of a new aziridinylbenzoquinone, RH1, as a NQO1-directed antitumor agent. Clin Cancer Res 1998;4(12):3083–8.

11. Sharp SY, Kelland LR, Valenti MR, Burunton LA, Hobbs S, Workman P. Establishment of an isogenic human colon tumor model for NQO1 gene expression: application to investigate the role of DT-diaphorase in bioreductive drug activation in vitro and in vivo. Mol Pharmacol 2000;58:1146–55.

12. Collard J, Matthew AM, Double JA, Bibby MC. EO9: relationship between DT-diaphorase levels and response in vitro and in vivo. Br J Cancer 1995;71:1199–203.

13. Siegel D, McGuinness SM, Winski SL, Ross D. Genotype-phenotype relationships in studies of a polymorphism in NAD(P)H:quinone oxidoreductase 1. Pharmacogenetics 1999;9:113–21.

14. Ernster L. DT-diaphorase Methods Enzymol 1967;10:309–17.

15. Benson AM, Hunkeler MJ, Talalay P. Increase of NAD(P)H:quinone reductase by dietary antioxidants: possible role in protection against carcinogenesis and toxicity. Proc Natl Acad Sci USA 1980;77: 5216–20.

16. Lowry OH, Rosebrough NJ, Farr AL, Randall RJ. Protein determination with the Folin phenol reagent. J Biol Chem 1951;193:265–75.

17. Vermilion JL, Coon MJ. Purified liver microsomal NADPH-cytochrome P-450 reductase. Spectral characterization of oxidation-reduction states. J Biol Chem 1978;253(8):2694–704.

18. Mihara K, Sato R. Detergent-solubilized NADH-cytochrome b5 reductase. Methods Enzymol 1978;52:102–8.

19. Sedlak J, Lindsay RH. Estimation of total, protein-bound, and nonprotein sulfhydryl groups in tissue with Ellman's reagent. Anal Biochem 1968;25(1):192–205.

20. Winski SL, Swann E, Hargreaves RH, et al. Relationship between NAD(P)H:quinone oxidoreductase 1 (NQO1) levels in a series of stably transfected cell lines and susceptibility to antitumor quinones. Biochem Pharmacol 2001;61(12):1509–16.

21. Ward TH, Butler J, Shahbakhti H, Richards JT. Comet assay studies on the activation of two diaziridinylbenzoquinones in K562 cells. Biochem Pharmacol 1967;53:1115–21.

22. Collins A, Dusinska M, Franklin M, et al. Comet assay in human biomonitoring studies: reliability, validation and applications. Environ Mol Mutagen 1997;30:139–46.

23. Lebailly P, Vigreux C, Godard T, et al. Assessment of DNA damage induced in vitro by etoposide and two fungicides (carbendazim and chlorothalonil) in human lymphocytes with the comet assay. Mutat Res 1997;375:205–17.

24. Kamer I, Rinkevich B. In vitro application of the comet assay for aquatic genotoxicity: considering a primary culture versus a cell line. Toxicol in Vitro 2002;12:177–84.

25. Patel V, Senderowicz AM, Pinto D Jr, et al. Flavopiridol, a novel cyclin-dependent kinase inhibitor, suppresses the growth of head and neck squamous cell carcinomas by inducing apoptosis. J Clin Investig 1998;102(9):1674–81.

26. Kruczynski A, Astruc J, Ricome C, Colpaert F, Hill BT. Definite antitumor activity of vinflunine, a novel fluorinated vinca alkaloid,

against human tumour xenografts. In: Fiebig HH, Burger AM, editors. Relevance of tumor models for anticancer drug development. Contributions oncology, vol. 54. Basel: Karger; 1999. p. 369–78.

27. Schwartz M. A biomathematical approach to clinical tumor growth. Cancer (Phila.) 1961;14:1272–94.

28. Cosaert J, Quoix E. Platinum drugs in the treatment of non-small-cell lung cancer. Br J Cancer 2002;87:825–33.

29. Tice RR, Agurell E, Anderson D, et al. Single cell gel/comet assay: guidelines for in vitro and in vivo genetic toxicology testing. Environ Mol Mutagen 2000;35:206–21.

30. Beall HD, Liu Y, Siegel D, Bolton EM, Gibson NW, Ross D. Role of NAD(P)H:quinone oxidoreductase (DT-diaphorase) in cytotoxicity and induction of DNA damage by streptonigrin. Biochem Pharmacol 1996;51(5):645–52.

31. Ross D, Beall H, Traver RD, Siegel D, Phillips RM, Gibson NW. Bioactivation of quinones by DT-diaphorase, molecular, biochemical, and chemical studies. Oncol Res 1994;6:493–500.

32. Paull K, Camalier R, Fitzsimmons SA, Lewis AD, Workman P, Grever M. Correlations of DT-diaphorase expression with cell sensitivity data obtained from the NCI human tumor cell line panel [abstract]. Proc Am Assoc Cancer Res 1994;35:369.

33. Pink JJ, Planchon SM, Tagliarino C, Varnes ME, Siegel D, Boothman DA. NAD(P)H:quinone oxidoreductase activity is the principal determinant of b-lapachone cytotoxicity. J Biol Chem 2000; 275:5416–24.

34. Klement G, Huang P, Mayer B, et al. Differences in therapeutic indexes of combination metronomic chemotherapy and an anti-VEGFR-2 antibody in multidrug-resistant human breast cancer xenografts. Clin Cancer Res 2002;8(1):221–32.

35. Cresteil T, Jaiswal AK. High levels of expression of the NAD(P)H: quinone oxidoreductase (NQO1) gene in tumor cells compared to normal cells of the same origin. Biochem Pharmacol 1991;42(5):1021–7.

36. Jarrett CM, Bibby MC, Phillips RM. Bioreductive enzymology of malignant and normal human tissues [abstract]. Proc Am Assoc Cancer Res 1998;39:429.

37. Ross D, Beall HD, Siegel D, Traver RD, Gustafson DL. Enzymology of bioreductive drug activation. Br J Cancer 1996;74:S1–8.

38. Stratford IJ, Workman P. Bioreductive drugs into the next millennium. Anti-Cancer Drug Des 1998;13:519–28.

39. Bolzan AD, Bianchi MS. Genotoxicity of streptonigrin: a review. Mutation Res 2001;488:25–37.

40. Paull K, Camalier R, Fitzsimmons SA, Lewis AD, Workman P, Grever M. Correlations of DT-diaphorase expression with cell sensitivity data obtained from the NCI human tumor cell line panel [abstract]]. Proc Am Assoc Cancer Res 1994;35:369.

41. Gustafson DL, Beall HD, Bolton EM, Ross D, Waldren CA. Expression of human NAD(P)H:quinone oxidoreductase (DT-diaphorase) in Chinese hamster ovary cells: effect on the toxicity of antitumor quinones. Mol Pharmacol 1996;50:728–35.

42. Hargreaves RHJ, O'Hare CC, Hartley JA, Ross D, Butler J. Cross-linking and sequence specific alkylation of DNA by aziridinylquinones. 3. Effects of alkyl substituents. J Med Chem 1999;42:2245–50.

43. Roth T, Burger AM, Dengler W, Willmann H, Fiebig HH. Human tumor cell lines demonstrating the characteristics of patient tumors as useful models for anticancer drug screening. In: Fiebig HH, Burger AM, editors. Relevance of tumor models for anticancer drug development. Contribution oncology, vol. 54. Basel: Karger; 1999. p. 145–56.

44. Phillips RM, Burger AM, Fiebig H-H, Double JA. Genotyping of NAD(P)H:quinone oxidoreductase (NQO1) in a panel of human tumor xenografts: relationship between genotype status, NQO1 activity and the response of xenografts to Mitomycin C chemotherapy in vivo. Biochem Pharmacol 2001;62:1371–7.

45. Faig M, Bianchet MA, Winski S, et al. Structure-based development of anticancer drugs: complexes of NAD(P)H:quinone oxidoreductase 1 with chemotherapeutic quinones. Structure 2001;9:659–67.

Clinical Cancer Research

Development of a New Isogenic Cell-Xenograft System for Evaluation of NAD(P)H:Quinone Oxidoreductase-Directed Antitumor Quinones: Evaluation of the Activity of RH1

Donna L. Dehn, Shannon L. Winski and David Ross

Updated version	Access the most recent version of this article at: http://clincancerres.aacrjournals.org/content/10/9/3147

Cited articles	This article cites 38 articles, 11 of which you can access for free at: http://clincancerres.aacrjournals.org/content/10/9/3147.full#ref-list-1
Citing articles	This article has been cited by 7 HighWire-hosted articles. Access the articles at: http://clincancerres.aacrjournals.org/content/10/9/3147.full#related-urls

E-mail alerts	Sign up to receive free email-alerts related to this article or journal.
Reprints and Subscriptions	To order reprints of this article or to subscribe to the journal, contact the AACR Publications Department at pubs@aacr.org.
Permissions	To request permission to re-use all or part of this article, use this link http://clincancerres.aacrjournals.org/content/10/9/3147. Click on "Request Permissions" which will take you to the Copyright Clearance Center's (CCC) Rightslink site.